pcim EUROPE

Modelling and Sizing Sensitivity Analysis of a Fully Renewable Energy-Based Electric Vehicle Charging Station Microgrid

Mobin Naderi[1], Diane Palmer[1], Maria N. Munoz[2], Yazan Al-Wreikat[3], Matthew Smith[1], Ewan Fraser[3], Erica E. F. Ballantyne[2], David A. Stone[1], Daniel T. Gladwin[1], Martin P. Foster[1]

[1] Department of Electronic and Electrical Engineering, University of Sheffield, Sheffield, UK

[2] Sheffield University Business School, University of Sheffield, UK

[3] School of Engineering, University of Southampton, Southampton, UK

Corresponding author: Mobin Naderi, m.naderi@sheffield.ac.uk

Speaker: David A. Stone, d.a.stone@sheffield.ac.uk

Abstract

This paper presents long-term modelling and second-by-second simulation of an autonomous microgrid (MG), including only renewable energy sources (RESs) and a hybrid energy storage system (HESS) as energy provider, and an electric vehicle (EV) Charge Station as a group load. The model uses forecast data for wind speed and solar radiation to provide wind turbine (WT) and photovoltaic (PV) generated powers, and statistical data for vehicles within a defined car park to model the EV demand. It is flexible and can support varying several planning parameters, e.g. varying sizes of WT and PV generation as well as various capacities of energy storage systems (ESSs). Therefore, in order to examine the impact of variations in RESs and ESS sizes, as well as the impact of EV demand uncertainties on the performance and efficiency of the MG, e.g. EV unmet energy, several sensitivity analyses are provided. Based on sensitivity analysis results, one can find reasonable ranges of MG module sizes, and make a decision for sizing of the overall system. For the case study represented here, results show that at least one WT is required, increasing PV panels is more effective to meet the midday EV load in at the target location, and a lower level of Li-ion ESS capacity is sufficient storage for the charging/discharging of the EVs.

1 Introduction

The United Kingdom (UK) government is set to end the sale of new petrol and diesel vehicles by 2030 and only allow the sales of zero-emissions vehicles from 2035 to reduce transport sector emissions [1]. Charging electric vehicles (EVs) from electricity networks powered by renewable energy has the potential to maximise the decarbonisation plan for road transport. As the number of EVs grow in the UK, the rise in charging infrastructure is projected to increase to meet the demand to charge these vehicles, reaching a minimum number of 300,000 public charging points by 2030 [2]. Nevertheless, some challenges, like grid demand increase and supplying EVs by fossil fuels via converting to electrical energy, increases the importance of grid-isolated renewable energy-based charging stations.

The solution proposed here is a fully grid-independent EV charging station powered exclusively by renewable energy. This solution is developed as part of Future Electric Vehicle Energy networks supporting Renewables (FEVER) project [3]. RES generation, such as by solar and wind, supply EV chargers via an off-vehicle energy store (OVES), containing at least one energy storage technology to provide a cost-effective alternative to a high power, high-cost grid connection. Future publications will describe more hybrid OVESs with multiple ESS technologies.

In design and construction of electrical systems, e.g. the FEVER microgrid (MG), sizing of elements, particularly large elements, has a significant importance. On the other hand, MG planning and element sizing studies require modelling of the systems. Although short-term electrical modelling of MGs is necessary for stability analysis, control design, and short-term performance validation, long-term modelling should be done for MG planning and element sizing to cope with inter-seasonal variations in generation, for example. In order to calculate a long-term model of MGs, their elements/modules should be modelled, i.e. RESs, the load demand, and ESSs.

Renewable power output may be modelled from weather data. Ground-based records at the site of interest are arguably the most accurate resource. The alternative, where these are not available, is measurements from satellite instruments. A full comparison is given by [4]. IEA-PVPS has published a report providing guidance on the choice of data provider and radiation model [5]. The algorithms which describe the conversion of solar radiation data via the photovoltaic process to electrical yield are covered by [6].

An explanation of how to model the power output of a wind turbine and an example calculation is given by [7]. Wind speed is conventionally measured at 10 m height by meteorological stations. Zhou et al detail the power law approach to simulating wind speed at turbine hub height [8]. The correlation between hub-height wind speed and wind turbine yield is modelled by power curves provided by turbine manufacturers. A complete review of power curve generation methods is given in [9].

EV charging/load modelling methods and fundamentals are reviewed in [10]. Although EV load profiles can be modelled using empirical data of EV fleets to study the load behaviour after EV fleet construction [11], it is not possible for planning studies, i.e. before fleet construction. In [12], EV load modelling is done using distribution functions of charging duration, charging start time, and transaction energy for eight different EV models, which is useful for planning and sizing studies.

ESSs can be modelled in several levels of detail and for different applications. Although voltage, current, and state of charge (SOC) need to be modelled via electrical relationships in short-term studies, state of health (SOH), SOC, and calendar/cycle ageing should be modelled through power flow relationships in long-term studies, e.g. ESS sizing and system planning [13]. More challenging topics are calendar and cycle loss modelling, where several theoretical, empirical, and semi-empirical [14] models have been presented in the literature. Theoretical models based on several complicated electro-chemical and physical relationships, and empirical models requiring long periods to obtain results of several experiments are useful for studies [15], where the focus is on ESS modelling details. However, in MG sizing studies, where several MG modules should be modelled, semi-empirical [13, 14], and validated simplified [16] models are much more useful, where less detailed models are used based on empirical parameters.

Sensitivity analysis is a common tool to depict nonlinear and multivariable relationships between important features and changeable parameters of a system, which has been used in various research areas of small and large-scale power systems, e.g. stability analysis [17], controller design, optimal planning [18], and techno-socio-economical sizing of MGs [19]. In this paper, sensitivity analysis is used for MG module sizing in an isolated renewable-based EV charging station. The first contribution of the paper is to provide data-driven long-term annual models for WT and PV energy generation units, and EV charging station load demand as well as validated power-in-power-out model for the HESS. The second contribution is to propose details of sensitivity analysis for making decisions around the MG sizing, and to provide results for a real case study.

Modelling of the EV charging station MG is discussed in Section 2. The methodology of sensitivity analysis for MG module sizing using a long-term model is provided in Section 3. Section 4 presents the results and relevant discussions, and Section 5 concludes the paper.

2 EV Charging Station Microgrid Modelling

Figure 1 Shows an energy-based schematic of the studied MG including EV demand, i.e. an EV charge station, wind energy generation using WTs, solar energy generation using PV panels, and a hybrid ESS (HESS). An energy management and measurement system is required to schedule charging/discharging of HESS based on the difference signal of generation and consumption powers. It also uses the data to size the model elements required for planning studies, and provides reports required for sizing and decision making, accordingly. This block needs instantaneous values of EV demand, WT and PV generation, current SOC, maximum allowable C-rate, and some other features of the ESS to function.

As an example, a site for the proposed MG has been established at a general outdoor car park in the UK. To this end, the weather data required for RES generation prediction is obtained at the target

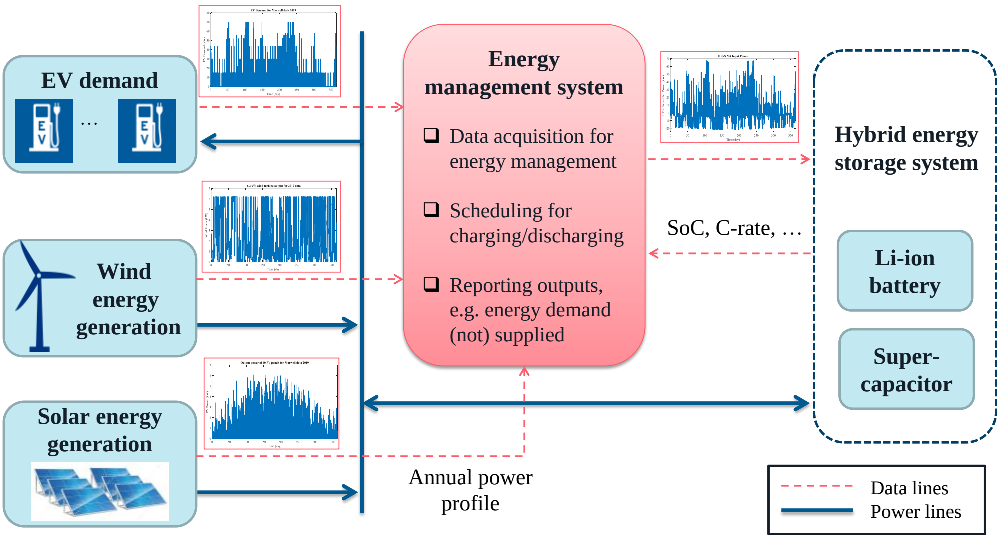

Fig. 1 An energy-based schematic of the studied MG useful in planning and sizing studies.

location in southern England, with a longitude 1.31° W and a latitude 51° N.

2.1 WT generation unit modelling

In order to calculate electrical yield, the input wind speed data is initially scaled to hub height. Since a relatively low wind turbine is to be employed here, the log law is applied because it is more reliable up to 20 m above the ground:

$$U_z = U_{z,ref} \times \ln\left(\frac{z}{z_0}\right) / \ln\left(\frac{z_{ref}}{z_0}\right), \quad (1)$$

where z and z_{ref} are new height (m) and reference height (m), respectively, and U_z and $U_{z,ref}$ are mean wind speed at the new height (m/s) and mean wind speed at the reference height (m/s), respectively. z_0 is surface roughness length (m). Surface roughness is a value based on protrusion of land cover e.g. grass, trees, buildings.

Calculation of wind yield i.e. power (kW) is achieved via interpolation of the manufacturer's power curve. The power curve is based on actual measurements. Interpolation supplies values which fall between measurements. Here, the power curve of Aventa AV-7 WT is used, which has a rated power as 6.2 kW [20].

2.2 PV generation unit modelling

The PV power output ($\mathrm{PV_{OUT}}$) has been obtained by transforming solar irradiance into power as follows:

$$\mathrm{P_{pv}}\ [\mathrm{kW}] = \mathrm{G_\beta} \times \eta_\mathrm{i} \times \eta_\mathrm{p} \times \mathrm{p_d} \times \mathrm{N_{pv}}, \quad (2)$$

where η_i is the inverter efficiency, η_p is the panel efficiency, $\mathrm{p_d}$ is the panel dimension $(\mathrm{m^2})$, and $\mathrm{G_\beta}$ is the solar irradiance on inclined surfaces $(\mathrm{kW/m^2})$.

$\mathrm{G_\beta}$ has been estimated by using a solar model developed in MATLAB. A detailed explanation of the development of the solar model can be found in [21] and in [22]. The input data for the model (i.e., global horizontal solar irradiation) was obtained through the Centre for Environmental Data Analysis (CEDA) archive. The hourly input data was measured at a weather station located in London between 2012 and 2019 in kJ/m^2.

2.3 EV load demand modelling

To determine the normal EV loading on the system it is possible to examine typical travel profiles for visitors to the selected location. In this case, the car park opens for visitors from 10 am until 5 pm, and this bounds when EVs can plug in and charge at the car park. The system is modelled using 10 uncontrolled AC chargers with a power rating of 7 kW each. The daily energy load demand for charging the EVs was calculated using the chargers' usage profile based on the total number of visitors arriving at the car park each day in 2019 and the hourly visitors' arrival profile. The model calculates the number of EVs arriving at the car park assuming four visitors per car arrive at the car park, with 3% of these cars being EVs.

Visitors typically park their cars for 4 hours while visiting the car park, used in this model as the plug-in period for each EV if any of the 10 chargers are free when arriving at the car park. The model assumes the average efficiency of an EV is 4 miles per kWh and needs to charge to cover a total distance of 30 miles. Figure 2 shows typical EVs behaviour at the car park and EV charging demand for a single day.

2.4 ESS modelling

Here, a general long-term model of ESSs is used, which is presented in detail, and is validated in [16]. It is a power-in-power-out model including parameters of SOC, SOH and degradation, a local logic-based ESS management system, charging/discharging losses, and import/export converter losses. Scheduled power of the ESS model, e.g. $P_{b,sch}$ for the Li-ion battery shown in Fig. 3, is obtained from the difference between the vehicle demand and the renewable generation. It can be either positive, meaning a load demand to discharge the ESS, or negative, which means a generation power to charge the ESS. When the SOC of the HESS is between its low and high limits, and the power demand does not lead to exceeding the maximum allowable c-rate of the ESS, the ESS can be charged or discharged successfully for the given scheduled power.

The ESS model can be generalised for different types of batteries, super-capacitors, and some other electrical and electro-chemical ESSs without any structural changes to the model, and only requiring reasonable parameters for each ESS technology. Table 1 shows the parameters for the

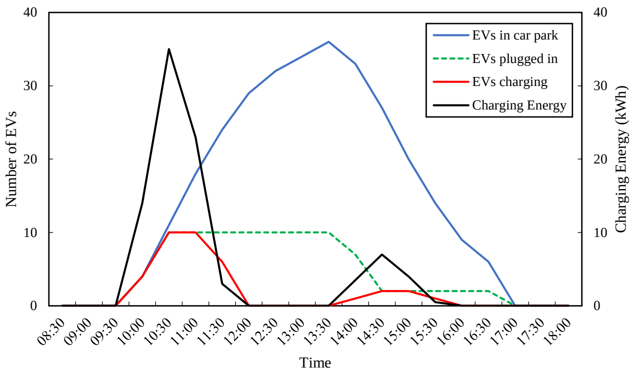

Fig. 2 EVs behaviour and load demand for an example day (20th of April).

ESS parameters	Battery value (unit)	Super-capacitor values (unit)
Nominal capacity	500 (kWh)	10 (kWh)
Initial capacity	500 (kWh)	10 (kWh)
Charging/discharging loss	3 (%)	3 (%)
Converter import/export loss	3 (%)	3 (%)
Maximum C-rate	1	10
SOC low limit	3 (%)	0 (%)
SOC high limit	97 (%)	100 (%)
Initial SOC	43 (%)	100 (%)
SOH loss per 1000 cycles	7 (%)	0.1 (%)
SOH calendar loss per month	0.5 (%)	0.005 (%)

Table 1 Hybrid ESS parameters and their values used in simulations.

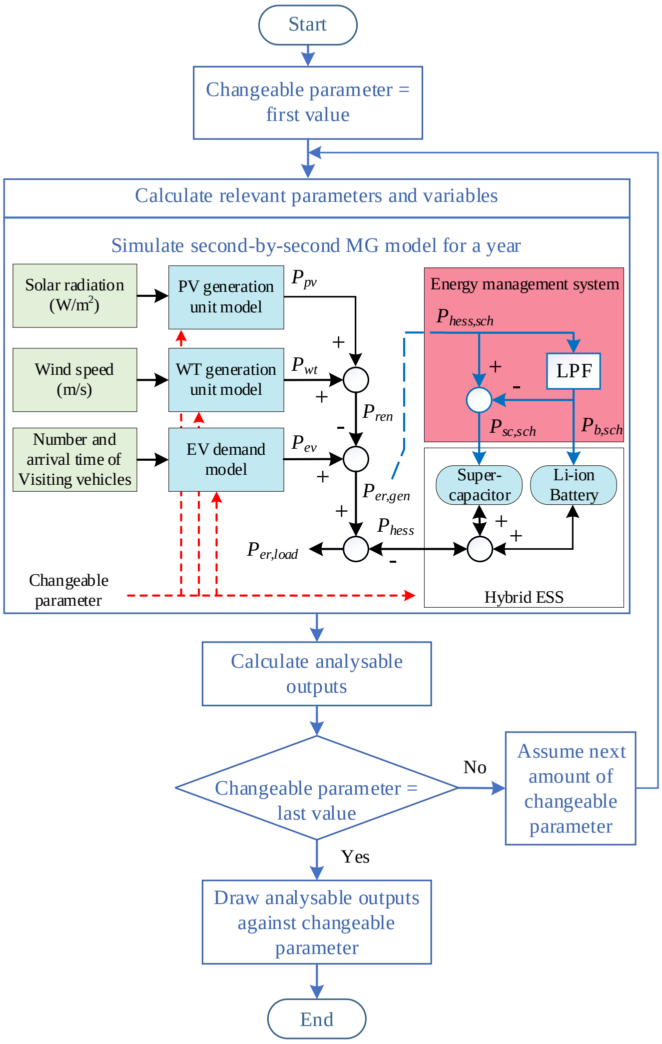

Fig. 3 Flowchart of the sensitivity analysis method used in MG module sizing.

studied hybrid ESS including the Li-ion battery and the super-capacitor.

A simple charging/discharging schedule is used in the energy management system according to a low-pass filter (LPF) performance such that slow charges/discharges are considered for the high-energy Li-ion battery ESS, and the high-power supercapacitor-based ESS is responsible for fast changes. The simulation part in Fig. 3 shows a schematic of the energy management system and the HESS modules inside the flowchart.

2.5 Overall Microgrid Modelling

After modelling the MG modules separately, they may be configured into the entire MG system. The simulation part in Fig. 3 shows the connections between different modules of the MG. According to the ESS/HESS model assumptions, the load demand is considered as positive, and the RES generation is denoted with negative values. The

RES generation power, P_{res}, is the sum of the WT generation power, P_{wt} and the PV generation power, P_{pv}. From this, it is possible to calculate the difference between the RES generation power and the EV demand power, P_{ev}, as follows:

$$P_{er,gen}(t) = P_{ev}(t) - P_{ren}(t). \quad (3)$$

where $P_{er,gen}$ is the generation error power. When its value is positive, it means the generation is not enough, and its negative value implies more generation power than the EV demand power. Assuming charging/discharging power of the HESS, P_{hess}, one can write the instantaneous power balance of the MG, as follows:

$$P_{er,load}(t) = P_{er,gen}(t) + P_{hess}(t). \quad (4)$$

where $P_{er,load}$ is the load error power. A positive value of the $P_{er,load}$ means EV demand power is not met, and a negative value of the $P_{er,load}$ means excess RES power neither consumed by the EV load nor stored in the HESS. Note that P_{hess} in Eq. (4) has positive values during discharging the HESS, and negative values during charging the HESS. The HESS power, P_{hess}, is obtained according to energy management system calculations for the HESS scheduled power, $P_{hess,sch}$.

The HESS scheduled power and the generation error power, i.e. $P_{hess.sch}$ and $P_{er.gen}$, are the same values (see Fig. 3). However, the generation error power and its equivalent energy are the actual power and energy signals, but the HESS scheduled power and its equivalent energy are control signals which are used in the energy management system. Note that the HESS scheduled energy and the generation error energy can be easily calculated by integrating $P_{hess,sch}$ and $P_{er,gen}$ with respect to time.

Figure 4 shows the annual power profile of $P_{hess,sch}$, where it is divided into two parts, i.e positive values as discharging power, $P_{hess,sch}^{dis}$, required for supplying remainder of the EV demand, and negative values as the charging power, $P_{hess,sch}^{ch}$, to store the excess RES power. The energy management system can be modelled as follows:

$$P_{b,sch}(t) = G_{lpf}(s) \times P_{hess,sch}(t), \quad (4a)$$
$$P_{sc,sch}(t) = (1 - G_{lpf}(s)) \times P_{hess,sch}(t), \quad (4b)$$

where $P_{b,sch}(t)$ and $P_{sc,sch}(t)$ are the scheduled powers of the Li-ion battery and super-capacitor, respectively. $G_{lpf}(s)$ is the LPF transfer function with ω_c as the cut of frequency as follows:

$$G_{lpf}(s) = \frac{\omega_c}{s+\omega_c}. \quad (5)$$

Finally, one can calculate the HESS power, according to the output powers of each ESSs as follows:

$$P_{hess,}(t) = P_{b,ex}(t) + P_{sc,ex}(t). \quad (6)$$

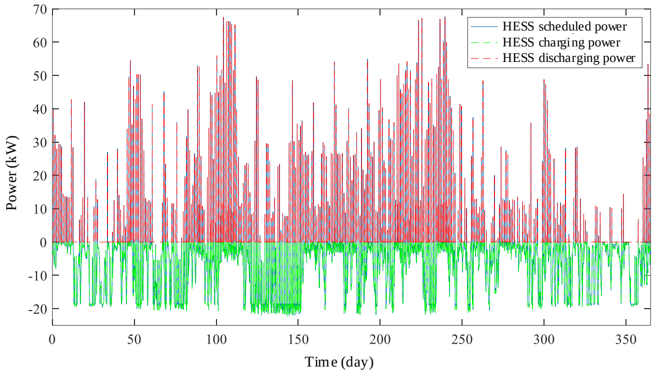

Fig. 4 Annual power profile of demand and generation difference as the HESS scheduled power (positive amounts for demand after subtracting the RES power and negative amounts for excess power of the RESs.

3 Sensitivity Analysis for MG Module Sizing

In the sensitivity analysis approach, there are two important concepts including a changeable parameter and an analysable variable. A changeable parameter is one of the parameters of the model, which is required to be changed to see the impact of these changes on the system performance. The performance is usually assessed using an (a few) output variable(s), which are valuable to be analysed, and can be called analysable variables. In this section, it is explained how the sensitivity analysis method is used to show the relationships between changeable parameters and analysable variables, which are important for module sizing. Since the analysable variables are selected to be different energy concepts in the MG, they are explained before the sensitivity analysis procedure.

3.1 Important energy concepts in MG sizing

MG sizing and planning require long-term calculations, where energy signals are more appropriate than power signals due to their cumulative feature with respect to the instantaneous power signals. Energy demand of the EV chargers, available RES energies, and HESS scheduled energy are the most important energy concepts to allow HESS scheduling by the energy management system. These can be obtained by integrating $P_{ev}(t)$, $P_{wt}(t)$, $P_{pv}(t)$, and $P_{hess,in}$ with respect to time.

Figure 5 shows annual energy profiles of the EV demand, one WT, 40 PV panels, and the HESS scheduled energy. The negative amount of the HESS scheduled energy shows that the available energy of the RESs is enough to meet the load demand if the generation and consumption times have enough overlap. However, both the EV demand in the car park and the RES generations have stochastic behaviours. Therefore, a negative HESS scheduled energy indicates enough excess RES energy generated to be able to charge the ESSs after supplying the vehicle charging load.

After scheduling the HESS, $P_{hess}(t)$ and $P_{er,load}(t)$ are important power signals. They include both positive and negative values as explained in Section 2.5, thereby these amounts should be separated before integrating them to calculate meaningful energy concepts as follows:

$$W_{hess,su} = \int P_{hess}^{+}(t)\,dt, \quad (7a)$$
$$W_{hess,st} = \int P_{hess}^{-}(t)\,dt, \quad (7b)$$
$$W_{ev,um} = \int P_{er,load}^{+}(t)\,dt, \quad (7c)$$
$$W_{gen,nst} = \int P_{er,load}^{-}(t)\,dt, \quad (7d)$$

where + and – denote positive and negative amounts, respectively. $W_{hess,su}$ is the energy supplied by the HESS, $W_{hess,st}$ is the stored energy in the HESS, $W_{ev,um}$ is the total EV demand unmet energy, and $W_{gen,nst}$ is the total excess generated energy of the RESs, which is not possible to be stored and/or consumed.

Although all these energy concepts are important in the MG sizing and planning, the HESS scheduled energy and the required energy to be supplied by HESS before scheduling the HESS, and energy supplied by the HESS and the EV demand unmet energy after scheduling the HESS are selected as analysable variables in the sensitivity analysis. Note that the required energy to be supplied by the HESS is calculated by integrating $P_{hess,sch}^{dis}$ with respect to time.

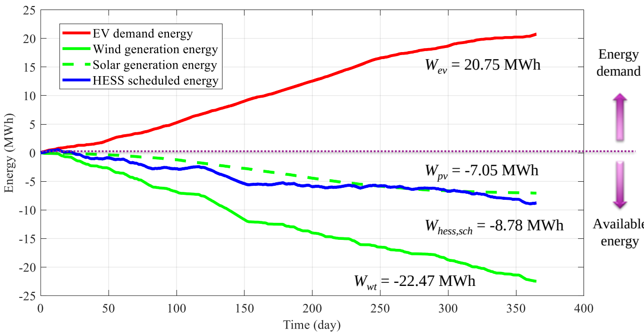

Fig. 5 Annual energy profiles of the EV demand, the WT, the PV panels, and the HESS scheduled energy.

3.2 Sensitivity analysis approach

Since the number of WT, number of PV panels, and ESS capacity need to be determined in the MG sizing, these are selected as changeable parameters. EV proportion is also selected as a changeable parameter to see the impact of EV demand fluctuations on the MG performance. Furthermore, as mentioned in the previous subsection, the HESS scheduled energy, the required energy to be supplied by the HESS, the energy supplied by the HESS, and the EV unmet energy are selected as analysable variables.

Figure 3 shows a flowchart diagram of the sensitivity analysis method used for the MG module sizing. Each changeable parameter includes a vector of a range of reasonable values. For each value, relevant parameters and variables in the MG model are updated, then the MG model is simulated second by second for the studied year and corresponding input data. The analysable outputs are calculated for each value, and after completing the process for all changeable parameter values, they will be drawn against the changeable parameter values.

4 Results and Discussion

The base case parameters used in simulations include 1 WT, 40 PV panels, and characteristics represented in Table 1 for the HESS. The area of the chosen PV panels is 1.67 m^2, ηi and ηp are assumed to be 78% and 12%, respectively. Moreover, EV proportion, number of EV chargers, the charger rated power, average EV park time, and EV average travel distance are assumed to be 3 %, 10, 7 kW, 4 h, and 48 km, respectively.

4.1 Sensitivity analysis for WT generation unit sizing

Figure 6 shows sensitivity analysis results for the number of wind turbines, between 0 and 3. As shown in Fig. 6(a), the HESS scheduled energy considerably increases in a negative direction with the increasing number of WTs. However, the energy required to be supplied by the HESS, shown by blue bars in Fig. 6(b), does not show a large decrease, which means a lot of the generated WT power is at different times from EV power demand. The orange bars show the total energy supplied by the HESS, which shows a large increase. Nevertheless, the EV unmet energy, shown by yellow bars, does not become zero even using three WTs. This is because the power profile of the EV demand and WT generation do not match. Therefore, having one WT is a reasonable choice, as the increase in the number of wind turbines from 0 to 1 gives a large decrease on the EV unmet energy, whilst a higher number of WTs may neither be technically reasonable nor cost-effective, as there are diminishing returns when considering the EV unmet energy.

4.2 Sensitivity analysis for PV generation unit sizing

Figure 7 shows sensitivity analysis results for PV panel number changeable between 0 and 50. By increasing the PV panel number, the HESS scheduled power, shown in Fig. 7(a), increases in negative values but in smaller steps with respect to the effect of a change in the number of WT. This increases the flexibility of the MG sizing. Figure 7(b) shows 3.35 MWh decrease, 2.95 MWh increase, and 6.3 MWh decrease in the required energy to be supplied by HESS, the HESS energy supplied, and the EV unmet energy, respectively. The EV unmet energy is considerably decreased by both increasing the PV generated power directly used to charge vehicles and increasing the charging/discharging of the HESS indirectly. It may be due to a better match between the solar power generation profile and the EV power demand profile when compared with the WT power profile. Therefore, increasing the PV panel number to improve the MG performance is more reasonable and provides better 'fine tuning' of the characteristics that is seen by increasing WTs.

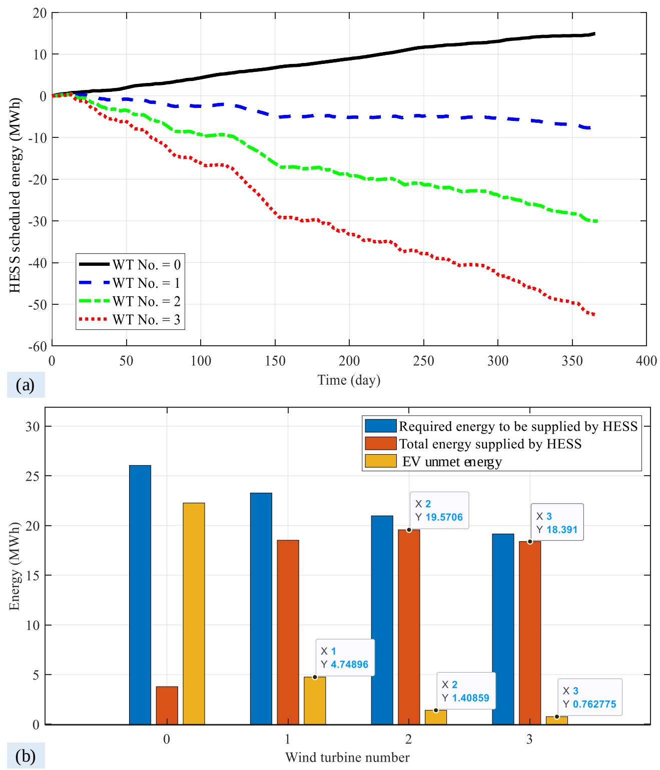

Fig. 6 Sensitivity analysis results of the WT number: (a) net input energy to the HESS, (b) required energy to be supplied by HESS, energy supplied by the HESS, and EV unmet energy.

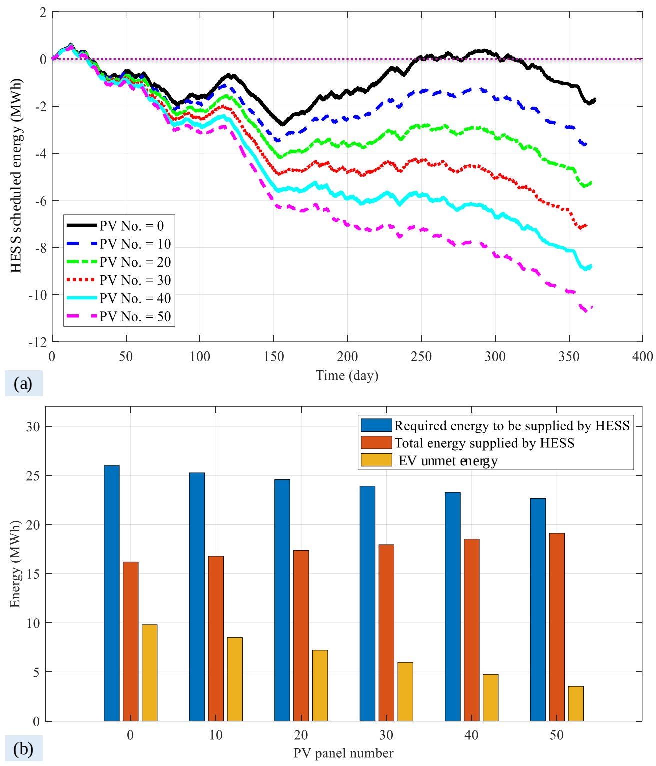

Fig. 7 Sensitivity analysis results of the PV panel number: (a) net input energy to the HESS, (b) required energy to be supplied by HESS, energy supplied by the HESS, and EV unmet energy.

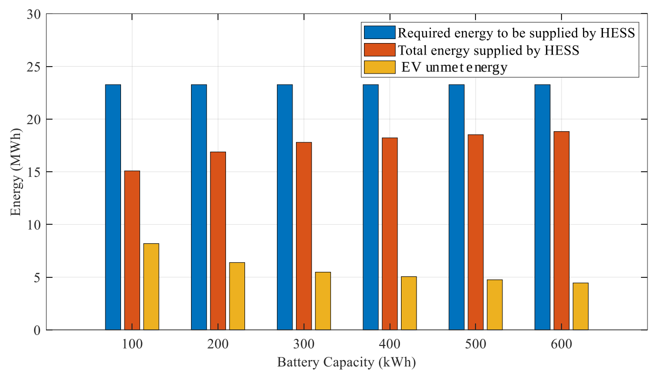

Fig. 8 Sensitivity analysis results of the ESS nominal capacity including required energy to be supplied by HESS, energy supplied by the HESS, and EV unmet energy.

4.3 Sensitivity analysis for ESS sizing

In this section, the sensitivity analysis is done for the Li-ion battery nominal capacity from 100 kWh to 600 kWh when the super-capacitor is disconnected. Since, the changeable parameter makes changes only on the output side of the HESS, the HESS input side energies do not change, e.g., the HESS scheduled energy and the required energy to be supplied by the ESS. Figure 8 shows an exponential behaviour for both the energy supplied by the HESS and the EV unmet energy.

In fact, they will be saturated for high amounts of the nominal capacity. Increasing the nominal capacity above 400 kWh does not lead to a significant decrease in the EV unmet energy. Therefore, the best size of the ESS should be in the lower band of the selected nominal capacity values.

4.4 Sensitivity analysis to study EV uncertainty

Since the number of EVs and their arrival time are stochastic, the load demand causes an uncertainty in long-term studies. Figure 9 shows required energy to be supplied by HESS, energy supplied by the HESS, and the EV unmet energy for different EV proportions as a metric of uncertainties. The MG needs more energy to be provided by the HESS when the EV proportion increases. However, RESs and the HESS sizes are assumed constant, which results in saturation of the total energy supplied by the HESS, and a linear increase in the EV unmet energy. In order to have a robust sizing approach, uncertainties should be included in sizing processes. In addition, a narrower band of uncertainties can be obtained by improving the model through adding details about the uncertain parameters as much as possible.

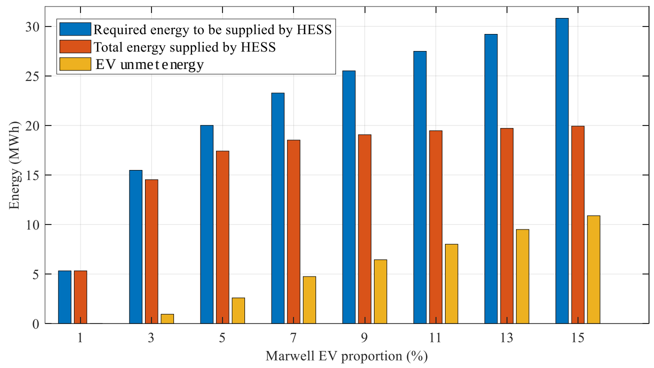

Fig. 9 Required energy to be supplied by HESS, energy supplied by the HESS, and EV unmet energy for different EV proportions.

5 Conclusion

Sensitivity analysis is a powerful, and at the same time simple, tool to inspect linear/nonlinear relationships between important features and effective parameters of a system. Here, it was employed on a long-term model of an electric vehicle charging station microgrid, composed of renewable energy generation resources, and a hybrid energy storage. Although having two or three wind turbines with 6.2 kW rated power results in very low EV unmet energy, the decrease with respect to having one wind turbine is not significant enough to encourage stakeholders to pay two to three times the cost of a single wind turbine. In fact, as a more flexible solution, such small amounts of EV unmet energies can be provided by increasing the number of solar panels. Furthermore, the results show that a nominal capacity in the range 100 kWh-200 kWh is the most suitable choice for the Li-ion battery pack, as increasing the nominal capacity above this level leads to a negligible decrease in the EV unmet energy, which is both technically and economically undesirable. In order to have a robust approach to microgrid module sizing, uncertainties, e.g. electric vehicle number, should be taken into account.

6 Acknowledgements

The authors acknowledge the financial support received from the Engineering and Physical Sciences Research Council (EPSRC) through Future Electric Vehicle Energy Networks supporting Renewables (FEVER) grant EP/W005883/1.

7 References

[1] 'Transport decarbonisation plan', UK Government, https://www.gov.uk/government/publications/transport-decarbonisation-plan, 2021.

[2] 'UK electric vehicle infrastructure strategy', UK Government,https://www.gov.uk/government/publications/uk-electric-vehicle-infrastructure-strategy, 2022.

[3] 'Future Electric Vehicle Energy netwoks supporting Renewables', https://www.fever-ev.ac.uk/, 2023.

[4] Palmer, D., Koubli, E., Cole, I., et al: 'Satellite or ground-based measurements for production of site specific hourly irradiance data: Which is most accurate and where?', Solar Energy, 2018, 165, pp 240-255.

[5] IEA-PVPS., 'Worldwide Benchmark of Modelled Solar Irradiance Data' (IEA-PVPS T16-05, 2023), pp 1-39.

[6] Koubli, E., Palmer, D. Rowley, P., et al: 'Inference of missing data in photovoltaic monitoring datasets', IET Renewable Power Generation, 2016, 10, (4), pp. 434-439.

[7] Ahammed, S.: 'Optimisation of Floating Horizontal Axis Wind Turbine (HAWT) Blades for Aerodynamic Performance Measurement', International Journal of Innovations in Engineering Research and Technology [IJIERT], 2021, 8, (6), pp 2394-3696.

[8] Zhou, X., Qin, J., Li, H.D., et al.:' A statistical method to construct wind speed at turbine height for study of wind power in China.', Theor Appl Climatol, 2020, 141, pp 419–432.

[9] Lydia, M., Kumar, S.S., Selvakumar, A.I., et al.: 'A comprehensive review on wind turbine power curve modeling techniques', Renewable and Sustainable Energy Reviews, 2014, 30, pp 452-460.

[10] Amara-Ouali, Y., Goude, Y., Massart, P., Poggi, J. M., & Yan, H. (2021). A review of electric vehicle load open data and models. *Energies*, *14*(8), 2233.

[11] Schäuble, J., Kaschub, T., Ensslen, A., Jochem, P., & Fichtner, W. (2017). Generating electric vehicle load profiles from empirical data of three EV fleets in Southwest Germany. *Journal of Cleaner Production*, *150*, 253-266.

[12] Uimonen, S., & Lehtonen, M. (2020). Simulation of electric vehicle charging stations load profiles in office buildings based on occupancy data. *Energies*, *13*(21), 5700.

[13] Mathews, I., et al.: 'Technoeconomic model of second-life batteries for utility-scale solar considering calendar and cycle aging', Applied energy, 2020, 269.

[14] Krupp, A., et al.: Calendar aging model for lithium-ion batteries considering the influence of cell characterization', Journal of Energy Storage, 2022, 45.

[15] Lewerenz, M., et al.: 'Systematic aging of commercial LiFePO4| Graphite cylindrical cells including a theory explaining rise of capacity during aging', Journal of Power Sources, 2017, 345, pp 254-263.

[16] Hutchinson, A.J. and Gladwin, D.T.: 'Verification and analysis of a Battery Energy Storage System model', Energy Reports, 2022, 8, pp 41-47.

[17] Naderi, M., et al.: 'Interconnected autonomous ac microgrids via back-to-back converters—Part II: Stability analysis', IEEE Transa. Power Electron., 2020, 35(11), pp 11801-11812.

[18] Naderi, M., Bahramara, S., Khayat, Y., Bevrani, H.: 'Optimal planning in a developing industrial microgrid with sensitive loads', Energy Reports, 2017, 3, pp 124-134.

[19] Rathore, A., Kumar, A., Patidar, N. P.: 'Techno-socio-economic and sensitivity analysis of standalone micro-grid located in Central India', International Journal of Ambient Energy, 2023, pp 1-22.

[20] 'Aventa AV-7 power curve', https://en.wind-turbine-models.com/turbines/ 1529-aventa-av-7.

[21] Nunez Munoz M, Ballantyne E.E.F, Stone D.A.: 'Development and evaluation of empirical models for the estimation of hourly horizontal diffuse solar irradiance in the United Kingdom', Energy, 2022, 241. https://doi.org/10.1016/j.energy.2021.122820.

[22] Nunez Munoz, M., Ballantyne, E.E.F. and Stone, D.A.: 'Assessing the Economic Impact of Introducing Localised PV Solar Energy Generation and Energy Storage for Fleet Electrification', Energies, 2023, 16(8), p 3570. doi:10.3390/en16083570.